Adhesive conductive hydrogels with wrinkled Janus surface and ultra-high sensitivity used as strain sensors

Yu Jiang
Donghua University
Wanqi Feng
Donghua University
Yixiang Chen
Donghua University
Wei Wang
Donghua University
Dan Yu (yudan@dhu.edu.cn)
Donghua University Songjiang Campus https://orcid.org/0000-0003-4166-8026

Research Article

Keywords: Conductive hydrogels, wrinkled structure, adhesion, high sensitivity, strain sensors

Posted Date: May 25th, 2022

DOI: https://doi.org/10.21203/rs.3.rs-1607290/v1

Abstract

Conductive hydrogels have attracted enormous attention in wearable electronic devices due to considerable flexibility and similarity with human skin. However, the majority of hydrogels were fabricated by one-pot process and were completely homogeneous, which limited the response to electrical signals. In this paper, we propose a simple strategy to obtain asymmetrical polyacrylic acid/chitosan@silver nanowires (PAA/CS@AgNWs) hydrogels, namely, depositing AgNWs layer by dropping AgNWs dispersions in ethanol on PAA/CS hydrogel prepared via one-pot process. Ethanol diffused into the hydrogel and endowed the upper surface with wrinkle structure. Besides, the inevitable conductivity difference between hydrogel itself and AgNWs further enhanced the sensitivity, leading to the ultra-high gauge factor (GF = 191.2, 7413, 18720). The adhesion of the hydrogel not only improved the adaptability to skin, but also the fastness of AgNWs. Reliable application performance (flexibility, self-healing, dry resistance and adhesion) and excellent electrical signal response (ultra-high sensitivity, identification, repetition and stability) indicated the potential applications in motion detection, gesture recognition and health monitoring.

1. Introduction

Recently, in order to meet the demand of personalized monitoring of physiological signals (heart-beating rate (Ye et al, 2020), movement (Wu et al, 2019) and vocalization (Pan et al, 2019)), abundant wearable devices have emerged in the market, such as smart glasses, smart watches and medical smart wristbands. However, the problems of uncomfortable wearing and poor adaptability to complex surfaces have not been solved yet. Nowadays, flexible wearable electronic devices (flexible sensors (Bao et al, 2021; Chen et al, 2020), implantable medical devices (Li et al, 2019; Zheng et al, 2019), bionic skin (Ma et al, 2019; Zheng et al, 2021), etc.) have attracted extensive attention due to their wearability, real-time feedback, remote control and other advantages (Huang et al, 2020). Acting as the indispensable unit of flexible wearable devices, flexible sensors, the component that can accept external stimuli (strain (Mao et al, 2020; Zha et al, 2020), pressure (Liu et al, 2020; Wang et al, 2021), temperature (Chen et al, 2021; Feng et al, 2021), humidity (Pan et al, 2020; Wu et al, 2019b) and gas (Wu et al, 2020; Wu et al, 2021)) and convert them into detectable electrical signals, overcome the rigidity of traditional metal-based or semiconductor-based sensors and exhibit higher flexibility, ductility and adaptability. Defined as flexible materials with three-dimensional porous structure and high-water content, hydrogels are similar to human skin in many aspects, hence they are widely application in the fields of drug carriers (Mandal et al, 2017) and tissue engineering (Henn et al, 2022). Additionally, conductive hydrogels are supposed to be desirable choice for sensors because of their excellent stretchability and biocompatibility, and yet the sensitivity of most hydrogel-based sensors is lower than that of others (fiber-based (Pan et al, 2020), elastomer-based (Gong et al, 2017; Zhang et al, 2020), mixed (Han et al, 2019)). Therefore, exploiting highly sensitive conductive hydrogels without sacrificing physical properties is of great significance to the promotion of flexible wearable devices.

Since all external stimuli are ultimately reflected in the form of electrical signals, the selection and distribution of conductive materials is the top priority of wearable sensors. Based on different conductive principles, the selectable conductive materials include ionic conductors (electrolyte (Chen et al, 2021; Liu et al, 2021; Lu et al, 2021), ionic liquid (Izawa et al, 2009; Lee et al, 2008)) and electronic conductors (intrinsic conductive polymer (Jiao et al, 2021; Zhou et al, 2021), carbon-based materials (Liao et al, 2019; Sun et al, 2021) and metal-based materials (Wang et al, 2019; Zhang et al, 2022)). Among them, AgNWs have attracted extensive attention because of their good conductivity and bactericidal properties (Pan et al, 2021). At present, conductive hydrogels are usually prepared by a simple one-pot process to obtain the homogeneous dispersion in the hydrogel (Chen et al, 2018; Hu et al, 2022; You et al, 2021). But it is not economical since a large number of conductive fillers are needed, and the cost problem is intensified when the expensive conductors like AgNWs and MXene are used. Moreover, electronic conductors tend to aggregate with the movement of water molecules, resulting in the deteriorated conductivity during long-term storage. The effect of conductive fillers on the mechanical properties and biocompatibility of hydrogels is also a latent question worth considering as well. The Janus structure (Zhao et al, 2017) can be obtained by depositing conductive materials on the upper surface of hydrogels, which not only can decrease the quantity of fillers, but also can enhance the sensitivity through the conductivity difference between the surface layer and the hydrogel itself. In view of strain sensors, the conductivity network varies with the overall stretch of the hydrogel, and the surface structure hardly affects the sensitivity for homogeneous hydrogels. For instance, Wang et al. (Wang et al, 2019) prepared a poly (3, 4-ethylenedioxythiophene): sulfonated lignin/PAA hydrogel and then succeed in constructing self-wrinkled structure by solvent replacement, but the improvement of GF was not obvious enough. However, the change of the surface structure for the stretched hydrogel with Janus structure will directly affect the conductive network, thereby improving the sensitivity of strain sensing.

As an all-in-one conductive hydrogel, the adhesion of conductive material and hydrogel body is important to the service life of the sensor. The conventional method is encapsulating to prevent the surface conductors from falling off, but the commonly used packaging materials such as PDMS (Gong et al, 2017) will greatly influence the sensitivity and extensibility of the hydrogels. To address the issue of good adhesion, the combination of fillers and polymer network by coordination bonds, hydrogen bonds or others interactions needs designing. Inspired by mussels, researchers found that substances with catechol structure (polydopamine (Rahim et al, 2016; Teixeira et al, 2012; Wu et al, 2020), tannic acid (He et al, 2021; Sun et al, 2021)) combine matrix via π-π interactions, metal coordination, covalent crosslinks and hydrogen bonds (Xie et al, 2020). The use of adhesive matrix materials is an easier method to make adhesive hydrogels, though the adhesion of these materials is relatively weak (Xia et al, 2019). Fu et al (Fu et al, 2021) and Lu et al. (Lu et al, 2020) prepared PAA/PEDOT hydrogels and PAA/CNS hydrogels respectively, and proved their adhesion. In addition, good adhesion is also conducive to tight fit between hydrogels and skins, so that their deformations are precisely matched and the accuracy of sensors reflecting physiological signal is improved (Pan et al, 2021; Sun et al, 2021).

Herein, we demonstrated a simple two-step method to fabricate hydrogel-based strain sensors with self-healing, water retention, and ultra-high sensitivity as flexible wearable devices. Briefly speaking, the

hydrogel body is comprised of PAA and CS via a one-pot process, and the wrinkled surface of AgNWs layer is obtained by simple dripping-drying (Fig. 1). The Janus structure and the conductivity difference between AgNWs and PAA/CS hydrogels endows the outstanding sensing sensitivity (GF = 191.2, 7413, 18720). In addition, the good self-adhesive of the PAA/CS hydrogel ensures the adhesive strength of the AgNWs and the precise matching of the sensor to external strain stimuli. Good physical properties and excellent sensing performance show the potential application in electronic skins, soft robots and interactive devices.

2. Experimental

2.1 Materials and chemicals

Acrylic acid (AA), ammonium persulfate (APS), acetic acid, glycerol, ethanol and $FeCl_3 \cdot 6H_2O$ were purchased from Sinopharm Chemical Reagent Co. Ltd. Chitosan (CS) was obtained from Shanghai San yuan Co. Ltd. AgNWs dispersion in ethanol (10 mg/ml) was commercially available from Tanfeng Tech. (Suzhou). Deionized (DI) water was used throughout the process unless otherwise specified.

2.2 Fabrication of PAA/CS@AgNWs hydrogels

PAA/CS hydrogels were prepared via a simple one-pot process. Specifically, CS (160 mg) and AA (16 ml) were added to a binary solvent consisting of DI water and glycerol. A trace of acetic acid was added to facilitate the dissolution and the mixed solution was magnetic stirred at 70 ℃ until completely dissolved. Unequal amounts of $FeCl_3$ (0.02, 0.04, 0.06, 0.08, 0.10 mol) and 1 mL APS solution (0.4 M) were mixed into above mixture to obtain uniform solutions. After removing bubbles in vacuum oven, 1.5 ml solution was poured into a mould sized 40 mm × 10 mm. Finally, thermally initiated radical polymerization led to the gelation of solution at 70 ℃ for 4 h and the PAA/CS hydrogel was obtained. Low concentrations (2, 4, 6, 8 mg/ml) AgNWs dispersions in ethanol were obtained by diluting 10 mg/ml AgNWs. All AgNWs dispersions needed ultrasonic treatment to make them disperse evenly. A total of 1 ml AgNWs dispersion was added dropwise to the PAA/CS hydrogel and dried to obtain the AgNWs/PAA/CS hydrogel with wrinkled Janus structure.

2.3 Measurements and Characterizations

The AgNWs/PAA/CS hydrogel was put in water for 72 h to exchange glycerol, and the water was dislodged by Vacuum Freeze Drier (FD-1F-50, China). The surface topography of the AgNWs/PAA/CS hydrogel was exhibited by scanning electron microscopy (SEM, TM-1000, Hitachi, Japan). The mechanical properties of hydrogels were tested by Universal Testing Machine (ZQ-990B, China). The square resistance was measured by Four-Point Probes (RTS-9, China). Measure the mass of hydrogels for different storage-time and the weight retention rate was calculated. The electrical signals varied with strain were gauged by Digital Multimeter (DMM6500, Keithley, USA). For further explanation, the relative resistance was defined as $(R - R_0)/R_0$, where R_0 and R represent the initial resistance and the real-time resistance.

3. Results And Discussions

3.1 Formation and micromorphology of the hydrogel

The preparation mechanism of the target PAA/CS@AgNWs hydrogel was shown in Fig. 1b. Acrylic acid (AA) monomers were polymerized by thermal initiation with oxidant APS to obtain PAA chains that were twined via coordination and electrostatic interaction with Fe^{3+} to form a three-dimensional (3D) network structure, which assured the shape stability of hydrogels. As a well-known biocompatible material, CS chains contain numerous -OH and -NH_2 groups, providing binding sites for hydrogen bonding with -COOH in PAA and further enhancing physical and mechanical properties of hydrogels. Afterwards, the AgNWs dispersion in ethanol was added in the upper surface of the PAA/CS hydrogels, and the AgNWs layer was deposited. As partial ethanol diffused into PAA/CS hydrogel, causing uneven swelling on the top surface and wrinkled structure that could be observed by naked eyes (Fig. 2a).

The optical image of the PAA/CS@AgNWs hydrogel prepared was showed in Fig. 2b. The PAA/CS hydrogel acted as a support for the AgNWs layer that was obvious observed in Fig. 2c. As shown in Fig. 2d and 2e, the PAA/CS hydrogel itself contained dense pores to form network structure, which proved the successful preparation of the PAA/CS@AgNWs hydrogel. Noticeably, the surface wrinkled structure was unable to be observed in the SEM images because the hydrogel is treated by solvent exchange before freezing and drying.

3.2 Mechanical properties

The reliable mechanical properties are the basis of normal work as a wearable device. Fe^{3+} was the crosslinking agent of PAA network that was the major component of the hydrogel, which mean the concentration of $FeCl_3$ had a significant effect on the mechanical properties of the PAA/CS@AgNWs hydrogel. A series of hydrogel samples with different $FeCl_3$ contents were prepared and used for investigation on tensile properties (Fig. 3a). Because of the low concentration of crosslinking agent, the solution with 0.01 M $FeCl_3$ could not be effectively shaped for stress-strain test. With increasing concentration of $FeCl_3$, more crosslinking points were obtained inside the hydrogel, resulting in a more compact cross-linking network and higher breaking strength. However, high crosslinking density limited the free slip of PAA chains, resulting in the breakage of hydrogel due to stress concentration. Therefore, 0.03 M $FeCl_3$ was chosen to further research. At this concentration, the Young's modulus of the hydrogel was 73.6 KPa, matching with that of the human skin (25–220 KPa) (Pan et al, 2020), which allowed the human body to move without feeling restricted and uncomfortable.

The PAA/CS@AgNWs hydrogel could be exposed to various complex working situations, including stretching (Fig. 3c), bending (Fig. 3d), twisting (Fig. 3e), and recovered after external force removal, which proved the excellent softness and elasticity. Otherwise, the hydrogel possessed considerable self-healing performance (Fig. 3f). After cutting and putting the two fracture surfaces of hydrogels in contact at 25 °C for 30 minutes, two pieces of hydrogel were reintegrated into one piece and could be stretched, although

the crack could still be observed. Since there was no irreversible covalent crosslinking in the hydrogel, the coordination, electrostatic and hydrogen bonds reformed when the cross section of the hydrogel was placed together, endowing the hydrogel excellent self-healing property.

3.3 Water retention and adhesion properties

As we know, high water content is an important feature of hydrogels. It is significant to retain water for a long-term storage to guarantee comfort and working stability. For the PAA/CS@AgNWs hydrogel, all ingredients except water would not lead to weight change at room temperature. Therefore, the weight retention rate could be used to represent water retention. The PAA/CS@AgNWs hydrogel was stored for 10 days and the weight was recorded at different days (Fig. 4a). After 10 days, the hydrogel maintained more than 87% weight, which indicated outstanding water retention. In the preparation process, part of the water had evaporated at 70 ℃, working like pre-drying effect. From the perspective of composition, glycerol is an excellent humectant and hygroscopic agent. The hydrogen bond between glycerol and water is stronger than that between water molecules, resulting in the decrease of the saturated vapor pressure and hard evaporation of water.

Adhesion properties are beneficial to the close bonding between hydrogel and skin, so that the deformation of them is accurately matched and correspondence between sensing signal and actual motion is guaranteed. The PAA/CS hydrogel was bonded to the surface of different materials, including rubber gloves (Fig. 4d), glass sheet (Fig. 4e), stainless steel ruler (Fig. 4f) and plastic ruler (Fig. 4g). The -COOH groups on PAA macromolecular chain were capable to form ionic bond, coordination bond or hydrogen bond with different surfaces and the -OH and -NH_2 groups on molecule acted as binding sites for hydrogen bonding, further improving the adhesion. Additionally, good flexibility maximized the contact area between hydrogel and complex interface. For the PAA/CS@AgNWs hydrogel, adhesion enhanced the fastness of the AgNWs layer on the upper surface, extending the service life as a wearable device.

3.4 Electrical properties

Because all external stimulation showed via electrical signals, electrical properties are crucial for strain sensors. Different concentration of AgNWs dispersions were added to the PAA/CS hydrogels, and the square resistance was recorded (Fig. 4b). Interestingly, the conductivity of PAA/CS hydrogel added 2 mg/ml AgNWs dispersions was poorer than PAA/CS hydrogel. Because the conductive pathway depended on the hydrogel itself instead of AgNWs on the surface which was too few to build a complete conductive network. However, the partial dispersant ethanol entered the PAA/CS hydrogel and inhibited the migration of electrolyte, resulting in the enlargement of square resistance. With the increasing concentration of AgNWs dispersions, the conductive pathway composed of AgNWs tended to be intact and the contact sites increased, which resulted in better conductivity. The 10 mg/ml AgNWs was chosen for further research because of the minimum resistance. As shown in Fig. 4c, the PAA/CS@AgNWs hydrogel, DC power and the light-emitting diode (LED) were connected to form a series circuit. When the hydrogel was stretched, the brightness of LED decreased significantly, intuitively reflecting the damage of

conductive path in the tensile direction. When the hydrogel was restored to its original length, the brightness of LED also recovered, which indicated the sensing performance and fatigue resistance.

3.5 Sensing performance and practical application

Undoubtedly, the sensing performance is of great significance to a wearable sensor. Defined as $(R-R_0)/R_0/\varepsilon$ (where R_0, R and ε mean the initial resistance, the real-time resistance and the strain respectively), GF is used to measure the sensitivity of the sensor. The dependent tendency of the relative resistance with strain of the PAA/CS@AgNWs hydrogel was shown in Fig. 5a, and the GF could be divided into three parts (= 191.2, 7413, 18720) and calculated by this graph. In the first stage, electrons transferred through AgNWs layer, and the resistance change resulted from the slip and crack of AgNWs. In the second stage, the crack in AgNWs layer was so large that the integrity of AgNWs could not be maintained. The transition of the conductive pathway from the silver nanowire layer on the upper surface to the hydrogel body remarkably. In the third stage, the AgNWs network was completely destroyed, and the hydrogel body was the conductive path, which meant that the stretching of hydrogel itself led to the transformation of electrical signal. By comparison, our work was much higher than the GF of the hydrogel-based sensors in recent years (as shown in Table 1). On the one hand, the wrinkled structure on the upper surface engendered more cracks of the AgNWs layer under the same strain, obtaining more obvious change in relative resistance and higher GF. On the other hand, the enormous discrepancy in conductivity between AgNWs layer and hydrogel itself played an important role to display the excellent sensitivity. The PAA/CS@AgNWs hydrogel also produced a certain response when bending deformation occurs. Analogous to the strain in tensile deformation, $(L_0-L)/L$ was used as the independent variable, where L represented the distance between the ends of the hydrogel and L_0 represented the original length. Obviously, the influence of electrical signal caused by bending was much lower than that by stretching.

Table 1
GF of the hydrogel-based sensors in recent years

Sample	Strain range	GF	Ref.
PAA/GO	5–50%	0.46	(Mao et al, 2020)
PVA/AgNWs	5–500%	0.58	(Azadi et al, 2020)
PVA/SNF/CN	0–100%	0.74	(Bao et al, 2021)
PVA/Gly/CNTs/CB	0–600%	2.07	(Gu et al, 2020)
PVA/rGO/GO	0–600%	2.10	(Chen et al, 2021)
PAM/gelatin	0–100%	2.5	(He et al, 2021)
PVA/P(AM-AA)	0–500%	2.74	(Huang et al, 2021)
	500–1000%	6.04	
PAA/GE/TA	0–600%	4.37	(Lu et al, 2020)
	600–1100%	7.6	
PAA/PEDOT:SL	0–100%	7	(Wang et al, 2019)
TOCNF/PAA/PANI	0–900%	8.0	(Jiao et al, 2021)
PAM/MMT/CNTs	0–1000%	2.77	(Sun et al, 2021)
	1000–4000%	5.17	
	4000– 4196%	8.5	
PVA/TA/PAM/AgNWs	0–700%	68.64	(Zhang et al, 2022)
PAA/carrageenan@CNTs	0–110%	343	(Han et al, 2020)
PAA/CS@AgNWs	0–40%	191.2	This work
	40–60%	7413	
	60–100%	18720	

Figure 5c revealed the relationship between relative resistance and small strain (1%, 2%, 5% and 10%). Figure 5d showed the electrical signal response at normal strain (10%, 20% and 30%). This meant that the PAA/CS@AgNWs hydrogel could guarantee the identification, repetition and stability of electrical signals facing with complex work conditions. Significantly, no perceptible wastage of electrical signal was discovered with the continuous loading-unloading cycle (5% for more than 200 times) as shown in Fig. 5e, indicating the reliable service life. Excellent sensitivity, signal repeatability and stability of the PAA/CS@AgNWs hydrogel were the basis of practical application in which stretching and bending always occurred at the same time. The PAA/CS@AgNWs hydrogel was placed on the index finger and wrist for practical application test. The resistance was the minimum in the initial state, and reached the maximum

when bending. When the index finger bent at different angles, the hydrogel presented distinguishable electrical signal responses, demonstrating the its potential application in motion tracking, health monitoring and other fields.

4. Conclusions

In summary, we designed the flexible, anti-drying and self-healing PAA/CS@AgNWs hydrogel based on non-covalent crosslinking. By dropping AgNWs dispersion in ethanol and drying, the AgNWs layer was successfully deposited and ethanol induced uneven swelling, causing the wrinkled structure on the upper surface. The wrinkled Janus structure and the electrical conductivity distinguishment between AgNWs and hydrogel itself led to ultra-high GF (= 191.2, 7413, 18720) compared with the recently reported hydrogels. Reliable adhesion ensured the seamless fit with the skin to accurately sense and promoted the fastness of AgNWs to extend the service life. Additionally, the PAA/CS@AgNWs hydrogel possessed identifiable, repeatable and stable electrical signal when strain occurred, which proclaimed the application prospect in wearable strain sensors.

Declarations

Funding

The authors declare that no funds, grants, or other support were received during the preparation of this manuscript.

Competing Interests

The authors have no relevant financial or non-financial interests to disclose.

Author Contributions

All authors contributed to the study conception and design. Material preparation, data collection and analysis were performed by Yu Jiang, Wanqi Feng and Yixiang Chen. The first draft of the manuscript was written by Yu Jiang and all authors commented on previous versions of the manuscript. All authors read and approved the final manuscript.

References

1. Azadi S et al (2020) Biocompatible and Highly Stretchable PVA/AgNWs Hydrogel Strain Sensors for Human Motion Detection. Adv Mater Technol-Us 5:2000426–2000437. DOI:10.1002/admt.202000426
2. Bao S et al (2021) Anti-freezing and antibacterial conductive organohydrogel co-reinforced by 1D silk nanofibers and 2D graphitic carbon nitride nanosheets as flexible sensor. Chem Eng J 411:128470–128482. DOI:10.1016/j.cej.2021.128470

3. Chen DJ et al (2020) Ultrastretchable, Tough, Antifreezing, and Conductive Cellulose Hydrogel for Wearable Strain Sensor. Acs Appl Mater Inter 12:53247–53256. DOI:10.1021/acsami.0c14935
4. Chen F et al (2018) Rational Fabrication of Anti-Freezing, Non-Drying Tough Organohydrogels by One-Pot Solvent Displacement. Angew Chem Int Ed Engl 57:6568–6571. DOI:10.1002/anie.201803366
5. Chen HJ et al (2021) High toughness multifunctional organic hydrogels for flexible strain and temperature sensor. J Mater Chem A 9:23243–23255. DOI:10.1039/d1ta07127k
6. Chen JW et al (2021) Tough and Antifreezing Organohydrogel Electrolyte for Flexible Supercapacitors with Wide Temperature Stability. Acs Appl Energ Mater 4:9353–9361. DOI:10.1021/acsaem.1c01556
7. Feng ZB et al (2021) Double Network Glycerol Gel: A Robust, Highly Sensitive, and Adaptive Temperature Sensor. Macromol Mater Eng 2100465–2100474. DOI:10.1002/mame.202100465
8. Fu F et al (2021) Interpenetrating PAA-PEDOT conductive hydrogels for flexible skin sensors. J Mater Chem C 9:11794–11800. DOI:10.1039/d1tc01578h
9. Gong XX et al (2017) Flexible strain sensor with high performance based on PANI/PDMS films. Org Electron 47:51–56. DOI:10.1016/j.orgel.2017.05.001
10. Gu JF et al (2020) Multifunctional Poly(vinyl alcohol) Nanocomposite Organohydrogel for Flexible Strain and Temperature Sensor. Acs Appl Mater Inter 12:40815–40827. DOI:10.1021/acsami.0c12176
11. Han JQ et al (2019) Nanocellulose-templated assembly of polyaniline in natural rubber-based hybrid elastomers toward flexible electronic conductors. Ind Crop Prod 128:94–107. DOI:10.1016/j.indcrop.2018.11.004
12. Han S et al (2020) Dual Conductive Network Hydrogel for a Highly Conductive, Self-Healing, Anti-Freezing, and Non-Drying Strain Sensor. Acs Appl Polym Mater 2:996–1005. DOI:10.1021/acsapm.9b01198
13. He Z, Yuan W (2021) Adhesive, Stretchable, and Transparent Organohydrogels for Antifreezing, Antidrying, and Sensitive Ionic Skins. ACS Appl Mater Interfaces 13:1474–1485. DOI:10.1021/acsami.0c18405
14. Henn D et al (2022) Enrichment of Nanofiber Hydrogel Composite with Fractionated Fat Promotes Regenerative Macrophage Polarization and Vascularization for Soft-Tissue Engineering. Plast Reconstr Surg 149:433e–444e. DOI:10.1097/PRS.0000000000008872
15. Hu JQ et al (2022) One-pot freezing-thawing preparation of cellulose nanofibrils reinforced polyvinyl alcohol based ionic hydrogel strain sensor for human motion monitoring. Carbohyd Polym 275:118697–118708. DOI:10.1016/j.carbpol.2021.118697
16. Huang JR et al (2021) Environment stable ionic organohydrogel as a self-powered integrated system for wearable electronics. J Mater Chem A 9:16345–16358. DOI:10.1039/d1ta03618a
17. Huang JR et al (2020) Self-powered integrated system of a strain sensor and flexible all-solid-state supercapacitor by using a high performance ionic organohydrogel. Mater Horiz 7:2085–2096.

DOI:10.1039/d0mh00100g

18. Izawa H et al (2009) Unique gel of xanthan gum with ionic liquid and its conversion into high performance hydrogel. J Mater Chem 19:6969–6972. DOI:10.1039/b916864h
19. Jiao Y et al (2021) Highly stretchable and self-healing cellulose nanofiber-mediated conductive hydrogel towards strain sensing application. J Colloid Interface Sci 597:171–181. DOI:10.1016/j.jcis.2021.04.001
20. Lee CK et al (2008) DNA hydrogel fiber with self-entanglement prepared by using an ionic liquid. Angew Chem Int Edit 47:2470–2474. DOI:10.1002/anie.200704600
21. Li H et al (2019) Fully Bioabsorbable Capacitor as an Energy Storage Unit for Implantable Medical Electronics. Adv Sci 6:1801625–1801633. DOI:10.1002/advs.201801625
22. Liao H et al (2019) Conductive MXene Nanocomposite Organohydrogel for Flexible, Healable, Low-Temperature Tolerant Strain Sensors. Adv Funct Mater 29:1904507–1904515. DOI:10.1002/adfm.201904507
23. Liu HY et al (2020) Freezing-Tolerant, Highly Sensitive Strain and Pressure Sensors Assembled from Ionic Conductive Hydrogels with Dynamic Cross-Links. Acs Appl Mater Inter 12:25334–25344. DOI:10.1021/acsami.0c06067
24. Liu J et al (2021) Ionic Conductive Organohydrogels with Dynamic Pattern Behavior and Multi-Environmental Stability. Adv Funct Mater 31:2101464–2101474. DOI:10.1002/adfm.202101464
25. Lu F et al (2020) Two-Dimensional Nanocellulose-Enhanced High-Strength, Self-Adhesive, and Strain-Sensitive Poly(acrylic acid) Hydrogels Fabricated by a Radical-Induced Strategy for a Skin Sensor. ACS Sustain Chem Eng 8:3427–3436. DOI:10.1021/acssuschemeng.9b07467
26. Lu J et al (2021) Highly tough, freezing-tolerant, healable and thermoplastic starch/poly(vinyl alcohol) organohydrogels for flexible electronic devices. J Mater Chem A 9:18406–18420. DOI:10.1039/d1ta04336f
27. Ma D et al (2019) Wearable, Antifreezing, and Healable Epidermal Sensor Assembled from Long-Lasting Moist Conductive Nanocomposite Organohydrogel. Acs Appl Mater Inter 11:41701–41709. DOI:10.1021/acsami.9b15412
28. Mandal B et al (2017) In Situ Silver Nanowire Deposited Cross-Linked Carboxymethyl Cellulose: A Potential Transdermal Anticancer Drug Carrier. Acs Appl Mater Inter 9:36583–36595. DOI:10.1021/acsami.7b10716
29. Mao J et al (2020) Highly stretchable, self-healing, and strain-sensitive based on double-crosslinked nanocomposite hydrogel. Compos Commun 17:22–27. DOI:10.1016/j.coco.2019.10.007
30. Pan W et al (2020) Facile Preparation of Highly Stretchable TPU/Ag Nanowire Strain Sensor with Spring-Like Configuration. Polymers-Basel 12:339–352. DOI:10.3390/polym12020339
31. Pan X et al (2019) An integrated transparent, UV-filtering organohydrogel sensor via molecular-level ion conductive channels. J Mater Chem A 7:4525–4535. DOI:10.1039/c8ta12360h

32. Pan XF et al (2020) An adaptive ionic skin with multiple stimulus responses and moist-electric generation ability. J Mater Chem A 8:17498–17506. DOI:10.1039/c9ta13407g
33. Pan Z et al (2021) Adhesive aero-hydrogel hybrid conductor assembled from silver nanowire architectures. Sci China Mater 64:2868–2876. DOI:10.1007/s40843-021-1677-3
34. Rahim MA et al (2016) Metal-Phenolic Supramolecular Gelation. Angew Chem Int Edit 55:13803–13807. DOI:10.1002/ange.201608413
35. Sun CY et al (2021) Ultra-stretchable, self-adhesive, transparent, and ionic conductive organohydrogel for flexible sensor. Apl Mater 9:011101–011111. DOI:10.1063/5.0035996
36. Sun D et al (2021) Ultrafast fabrication of organohydrogels with UV-blocking, anti-freezing, anti-drying, and skin epidermal sensing properties using lignin-Cu2 + plant catechol chemistry. J Mater Chem A 9:14381–14391. DOI:10.1039/d1ta02139g
37. Sun HL et al (2021) Environment Tolerant Conductive Nanocomposite Organohydrogels as Flexible Strain Sensors and Power Sources for Sustainable Electronics. Adv Funct Mater 31:2101696–2101706. DOI:10.1002/adfm.202101696
38. Teixeira LSM et al (2012) Enzyme-catalyzed crosslinkable hydrogels: Emerging strategies for tissue engineering. Biomaterials 33:1281–1290. DOI:10.1016/j.biomaterials.2011.10.067
39. Wang J et al (2021) "Crocodile skin" ultra-tough, rapidly self-recoverable, anti-dry, anti-freezing, MoS2-based ionic organohydrogel as pressure sensors. Colloid Surf A 625:126458–126468. DOI:10.1016/j.colsurfa.2021.126458
40. Wang LY, Daoud WA (2019) Hybrid conductive hydrogels for washable human motion energy harvester and self-powered temperature-stress dual sensor. Nano Energy 66. DOI:10.1016/j.nanoen.2019.104080
41. Wang Q et al (2019) Biocompatible, self-wrinkled, antifreezing and stretchable hydrogel-based wearable sensor with PEDOT:sulfonated lignin as conductive materials. Chem Eng J 370:1039–1047. DOI:10.1016/j.cej.2019.03.287
42. Wu J et al (2020) Stretchable, Stable, and Room-Temperature Gas Sensors Based on Self-Healing and Transparent Organohydrogels. Acs Appl Mater Inter 12:52070–52081. DOI:10.1021/acsami.0c17669
43. Wu J et al (2019a) Ultrastretchable and Stable Strain Sensors Based on Antifreezing and Self-Healing Ionic Organohydrogels for Human Motion Monitoring. Acs Appl Mater Inter 11:9405–9414. DOI:10.1021/acsami.8b20267
44. Wu J et al (2019b) An intrinsically stretchable humidity sensor based on anti-drying, self-healing and transparent organohydrogels. Mater Horiz 6:595–603. DOI:10.1039/c8mh01160e
45. Wu XX et al (2020) A wearable, self-adhesive, long-lastingly moist and healable epidermal sensor assembled from conductive MXene nanocomposites. J Mater Chem C 8:1788–1795. DOI:10.1039/c9tc05575d
46. Wu Z et al (2021) Conductive Hydrogel- and Organohydrogel-Based Stretchable Sensors. ACS Appl Mater Interfaces 13:2128–2144. DOI:10.1021/acsami.0c21841

47. Xia S et al (2019) Highly sensitive and wearable gel-based sensors with a dynamic physically cross-linked structure for strain-stimulus detection over a wide temperature range. J Mater Chem C 7:11303–11314. DOI:10.1039/c9tc03475g
48. Xie C et al (2020) Mussel-Inspired Hydrogels for Self-Adhesive Bioelectronics. Adv Funct Mater 30:1909954–1909983. DOI:10.1002/adfm.201909954
49. Ye Y et al (2020) Cellulose Nanofibrils Enhanced, Strong, Stretchable, Freezing-Tolerant Ionic Conductive Organohydrogel for Multi-Functional Sensors. Adv Funct Mater 30:2003430–2003441. DOI:10.1002/adfm.202003430
50. You Z et al (2021) One-pot synthesis of multi-functional cellulose-based ionic conductive organohydrogel with low-temperature strain sensitivity. Carbohydr Polym 251:117019–117028. DOI:10.1016/j.carbpol.2020.117019
51. Zha XJ et al (2020) Nanofibrillar Poly(vinyl alcohol) Ionic Organohydrogels for Smart Contact Lens and Human-Interactive Sensing. Acs Appl Mater Inter 12:23514–23522. DOI:10.1021/acsami.0c06263
52. Zhang L et al (2022) Neuron-inspired multifunctional conductive hydrogels for flexible wearable sensors. J Mater Chem C 4327–4335. DOI:10.1039/d1tc05864a
53. Zhang YL et al (2020) Highly Sensitive, Low Hysteretic and Flexible Strain Sensor Based on Ecoflex-AgNWs- MWCNTs Flexible Composite Materials. Ieee Sens J 20:14118–14125. DOI:10.1109/Jsen.2020.3008159
54. Zhao L et al (2017) Programmable and Bidirectional Bending of Soft Actuators Based on Janus Structure with Sticky Tough PAA-Clay Hydrogel. Acs Appl Mater Inter 9:11866–11873. DOI:10.1021/acsami.7b00138
55. Zheng S et al (2021) Moisture-wicking, Breathable and Intrinsically Antibacterial Electronic Skin Based on Dual Gradient poly(ionic liquid) Nanofiber Membranes. Adv Mater: e2106570. DOI:10.1002/adma.202106570
56. Zheng T et al (2019) Biocompatible Carbon Nanotube-Based Hybrid Microfiber for Implantable Electrochemical Actuator and Flexible Electronic Applications. Acs Appl Mater Inter 11:20615–20627. DOI:10.1021/acsami.9b02927
57. Zhou X et al (2021) Polyaniline-coated cotton knitted fabric for body motion monitoring. Sens Actuators A: Phys 321:112591–112601. DOI:10.1016/j.sna.2021.112591

Figures

Figure 1

a Fabrication of wearable strain sensor based on PAA/CS@ AgNWs hydrogel. **b** Fabrication mechanism of the hydrogel

Figure 2

a Ethanol induced wrinkled structure on the upper surface of the hydrogels. **b** A optical image of the PAA/CS@AgNWs hydrogel. SEM images of **c** AgNWs layer, and **d**, **e** the hydrogel itself

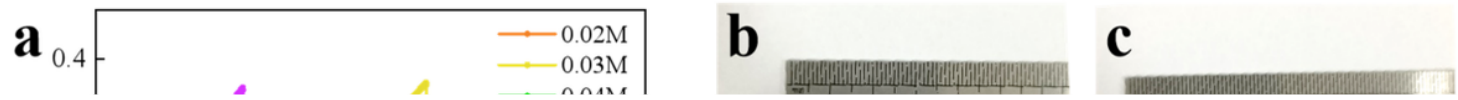

Figure 3

a Stress-strain curves of hydrogels with different concentration of $FeCl_3$. The hydrogel showed excellent flexibility and elasticity **b** initial state, **c** stretching, **d** bending and **e** twisting. **f** Self-healing performance

Figure 4

a Weight change of the PAA/CS@AgNWs hydrogel after storing for at 28°C for 30 days. **b** Electrical conductivity of hydrogels with different concentration of AgNWs. **c** In a series circuit, the brightness change of LED when the PAA/CS@AgNWs hydrogel was stretching and releasing. The adhesion between hydrogel and other materials **d** rubber, **e** glass, **f** steel and **g** plastic

Figure 5

The sensitivity of the hydrogel when **a** stretching and **b** bending. **c** The relationship between relative resistance and small strain (1%, 2%, 5% and 10%) and **d** the electrical signal response at normal strain (10%, 20% and 30%). **e** Electrical signal with the repetitive loading-unloading cycle. Application properties test **f** fingers bent for 30°, 60° and 90° and **g** wrist bent.